Journal of Medicinal Chemistry

ARTICLE

pubs.acs.org/jmc

Identification, Characterization, and Implications of Species-Dependent Plasma Protein Binding for the Oral Hedgehog Pathway Inhibitor Vismodegib (GDC-0449)

Anthony M. Giannetti, Harvey Wong, Gerrit J. P. Dijkgraaf, Erin C. Dueber, Daniel F. Ortwine, Brandon J. Bravo, Stephen E. Gould, Emile G. Plise, Bert L. Lum, Vikram Malhi, and Richard A. Graham*

Genentech Inc., 1 DNA Way, South San Francisco, California 94080, United States

ABSTRACT: Vismodegib (GDC-0449) is is an orally available selective Hedgehog pathway inhibitor in development for cancer treatment. The drug is ≥95% protein bound in plasma at clinically relevant concentrations and has an approximately 200-fold longer single dose half-life in humans than rats. We have identified a strong linear relationship between plasma drug concentrations and α-1-acid glycoprotein (AAG) in a phase I study. Biophysical and cellular techniques have been used to reveal that vismodegib strongly binds to human AAG (K_D = 13 μM) and binds albumin with lower affinity (K_D = 120 μM). Additionally, binding to rat AAG is reduced ~20-fold relative to human, whereas the binding affinity to rat and human albumin was similar. Molecular docking studies reveal the reason for the signficiant species dependence on binding. These data highlight the utility of biophysical techniques in creating a comprehensive picture of protein binding across species.

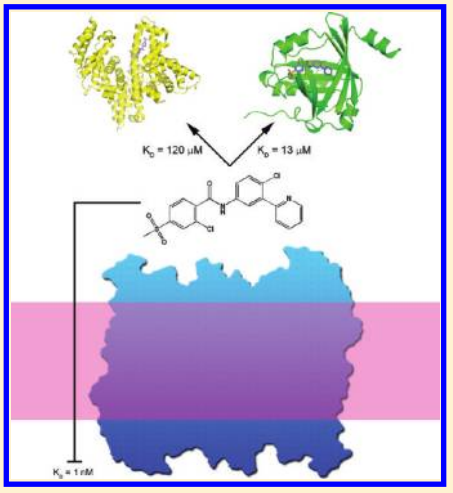

INTRODUCTION

The Hedgehog (Hh) signaling pathway plays a crucial role in human embryogenesis but is largely inactive in adult tissues under normal conditions. Aberrant Hh pathway activation has been implicated in a range of human cancers, and the targeting of this pathway as an anticancer strategy has been reported.[1,2] Vismodegib (GDC-0449, (2-chloro-*N*-(4-chloro-3-(pyridin-2-yl)phenyl)-4-(methylsulfonyl)benzamide) is a small-molecule, selective Hh pathway inhibitor (HPI) that is in phase II development for the treatment of various cancers including advanced basal cell carcinoma. Vismodegib targets a central mediator of Hh pathway signaling, the transmembrane protein Smoothened (SMO).[2−5] In the absence of ligand, SMO is inhibited by the Hh receptor Patched (PTCH). This inhibition is normally released when Hh binds to PTCH, but inappropriate activation of this pathway occurs in the presence of inactivating PTCH mutations or activating SMO mutations. Once activated, SMO initiates an intracellular signaling cascade that results in activation of transcription factors and expression of Hh target genes essential for cellular growth, differentiation, and survival. Vismodegib is able to inhibit both ligand-dependent and mutationally driven SMO-mediated signaling.[6]

Preclinical pharmacokinetic (PK) studies have demonstrated that vismodegib has moderate to low in vivo clearance, good oral bioavailability across animal species, and high metabolic stability in vitro, with nearly 100% of the compound remaining following incubation with human hepatocytes.[7] Preclinical in vitro studies also demonstrated that vismodegib is highly protein bound (≥95%) across species, including in human plasma at clinically relevant concentrations.[7] Despite the prediction of favorable human PKs based on the preclinical PKs of vismodegib, during a single dose study in healthy volunteers, vismodegib exhibited unexpectedly high plasma exposures coupled with an extremely low apparent oral clearance and a long half-life of approximately 10−14 days.[8] This half-life was substantially longer in comparison to rats in which half-life was approximately 1.5 h.[7,8] It is known that plasma protein binding is a contributing determinant of PK properties such as systemic clearance and volume of distribution for low clearance compounds and can influence the pharmacodynamics (PD) of pharmaceutical agents, including anticancer agents such as docetaxel,[9] erlotinib,[10] gefitinib,[11] imatinib,[12] and UCN-01.[13,14] Therefore, on the basis of the known potential impact of extensive protein binding on PKs and therapeutic potential, we initiated a more detailed investigation of the clinical and biochemical protein binding profile of vismodegib to better understand the unusual disposition of this compound.

We report here a detailed study of the interactions of vismodegib with α-1-acid glycoprotein (AAG) and serum

Received: July 15, 2010
Published: March 25, 2011

dx.doi.org/10.1021/jm1008924 | *J. Med. Chem.* 2011, 54, 2592–2601

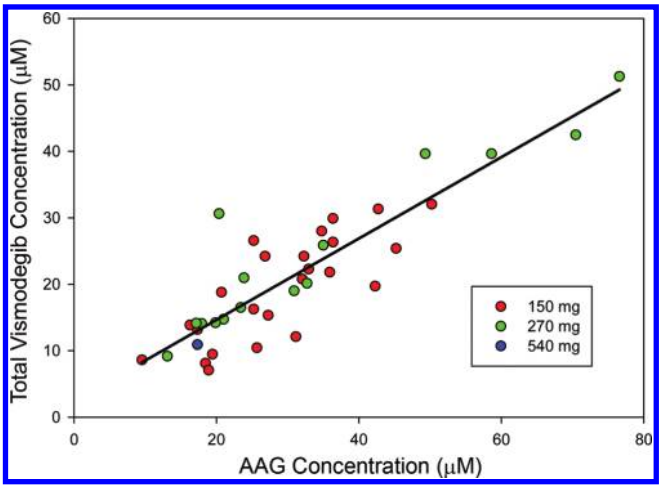

Figure 1. Correlation between vismodegib and AAG concentrations in patients with advanced cancers following 21 days of daily dosing of vismodegib. Slope of drawn line is 0.612; $R^2 = 0.78$.

albumin. These two proteins are the principal plasma components responsible for binding xenobiotics.[15] Analysis of plasma samples from 40 patients dosed with vismodegib to steady state revealed a strong correlation between the total concentration of drug in plasma and the plasma concentration of AAG (Figure 1). Serum albumin concentration is relatively constant over time in the absence of significant disease, whereas AAG levels can fluctuate more quickly and significantly, usually in response to inflammation.[16] The strong correlation between vismodegib and AAG concentrations suggests that AAG binding may be high affinity and is a determinant of total plasma concentration of vismodegib in patients. Therefore, changes in AAG levels could impact systemic concentrations of vismodegib. In addition, as total concentrations of vismodegib are influenced by AAG, flutuations in AAG levels have an impact on vismodegib pharmacodynamics.

To address these issues, we performed in vitro equilibrium binding and cell-based inhibition assays in the presence of different amounts of human AAG (hAAG). We confirmed vismodegib binds hAAG and can influence the effect of the drug as evidenced by a reduction of inhibition in a cell-based reporter assay. We then used surface plasmon resonance (SPR) and isothermal titration calorimetry (ITC) binding assays on human and rat AAG (rAAG) and albumin to investigate in detail the kinetics, thermodynamics, and species differentiation of binding. These studies revealed that vismodegib binding to both rat and human serum albumin is low affinity. In contrast, vismodegib binding to AAG exhibited high affinity to hAAG and low affinity in the case of rAAG. Molecular docking of vismodegib into the AAGs reveals a possible mechanism for this species-dependent binding. Implications for the relevance of these observations in patients are also discussed.

RESULTS

Correlation between Vismodegib and AAG Plasma Concentrations. In a phase I, first-in-man dose-escalation study, 40 patients with advanced cancer received 150, 270, or 540 mg/day vismodegib, plasma samples were collected 21 days after initiation of daily dosing, and AAG and vismodegib concentrations were determined. Linear regression revealed a strong correlation ($R^2 = 0.78$, slope = 0.61) between the total plasma concentrations of vismodegib and AAG (Figure 1). The same linear relationship was found for all three dose levels with a slope less than unity, suggesting that not all AAG binding sites are drug bound. These data predict that the steady-state plasma concentration of vismodegib is primarily determined by the amount of AAG present, which can fluctuate in response to changes in disease state, for example, in patients undergoing treatment with anti-HIV medications.[17]

Table 1. Concentration Grid of AAG and Vismodegib Binding by Equilibrium Dialysis[a]

	AAG concentration (% bound)		
vismodegib (μM)	0.5 mg/mL (10 μM)	1 mg/mL (20 μM)	5 mg/mL (100 μM)
5	96.5 ± 0.189	98.3 ± 0.143	98.8 ± 0.0485
25	70.4 ± 2.09	88.9 ± 0.236	98.7 ± 0.0509
75	41.1 ± 0.744	60.0 ± 0.674	98.3 ± 0.0236

[a] Data were fit to a binding model (see methods section) and indicate a K_D of 1.5 μM.

In Vitro Equilibrium Dialysis Binding between Vismodegib and AAG. We assessed vismodegib binding to hAAG using equilibrium dialysis. We measured binding at vismodegib concentrations of 5, 25, and 75 μM and hAAG concentrations of 0.5, 1, and 5 mg/mL. We found that binding to hAAG is saturable in vitro at clinically relevant concentrations of vismodegib and physiologically relevant concentrations of hAAG (Table 1) and that binding to hAAG is not saturable when hAAG concentrations are increased beyond normal levels[16] up to 5 mg/mL. A binding model (see Experimental Section) was fitted to the nine %-bound data points to estimate a dissociation constant (K_D) of 1.5 μM for the hAAG/vismodegib interaction (Table 1), which is quite strong relative to most drugs known to bind AAG.[18]

hAAG Impedes the Hh Pathway Inhibitory Activity of Vismodegib in Vitro. High-affinity binding of compounds by plasma proteins can attenuate the efficacy of the drug by preventing it from interacting with the intended target. Therefore, we examined the effect of the ability of vismodegib to inhibit Hh signaling in S12 cells in the presence of varying concentrations of hAAG (Figure 2). S12 cells are derived from the mouse embryonic fibroblast cell line C3H10T$^1/_2$ and have a *GLI*-luciferase reporter stably integrated in their genome so that Hh signaling can be monitored optically.[3] We chose to analyze the effect of medium supplemented with 0.5, 1.0, and 5.0 mg/mL hAAG to cover the range of AAG concentrations tested in the equilibrium dialysis. As previously reported,[6] the half-maximal concentration (IC_{50}) of vismodegib to inhibit Shh-induced *GLI*-luciferase reporter activity in the absence of hAAG is approximately 15 nM. Addition of 0.5 mg/mL hAAG reduced inhibition of Hh signaling more than 100-fold ($IC_{50} \approx 1750$ nM). Doubling the amount of hAAG in the medium to 1 mg/mL further reduced the IC_{50} of vismodegib, whereas no inhibition of *GLI*-luciferase activity was observed in the presence of 5 mg/mL hAAG, even at concentrations as high as 3 μM vismodegib. These results demonstrate that only free vismodegib can inhibit Hh signaling in vitro. In addition, while the presence of hAAG attenuates the observed IC_{50} in these assays, vismodegib remains effective over the range of physiological hAAG concentrations, only failing to produce observable inhibition in these experiments at a hAAG

dx.doi.org/10.1021/jm1008924 |J. Med. Chem. 2011, 54, 2592–2601

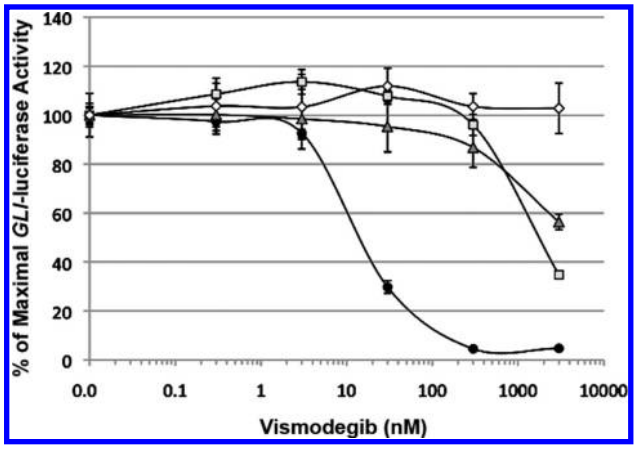

Figure 2. *GLI*-luciferase reporter activity of S12 cells stimulated with 200 ng/mL Shh in the absence (solid circles) or presence of 0.5 mg/mL (gray square), 1 mg/mL (gray triangle), or 5 mg/mL (white diamond) hAAG. Error bars indicate SD.

concentration that well exceeds the highest observed AAG concentration in patients in the phase 1 study.

Affinity and Kinetic Characterization of the Interaction between Vismodegib, AAG, and Serum Albumin. SPR binding assays can provide information about real-time association and dissociation[19] events between a compound and protein and were used to investigate the nature of the binding kinetics and reversibility of the interactions of vismodegib with plasma proteins. SPR assays, using Biacore technology, have a reasonably high throughput rate (~50 (samples/machine)/day) and can evaluate multiple proteins simultanesouly. Thus, we investigated vismodegib binding to hAAG and rAAG, as well as human and rat serum albumin (HSA and RSA, respectively), to assess (1) whether there is species dependence in binding, (2) whether albumin plays a significant role in the high degree of vismodegib plasma binding, and (3) whether the binding to either plasma protein is rapidly or slowly reversible, as slow reversibility has been observed to negatively affect other drugs in vivo.[13,14] The SPR assays were also performed at two temperatures. The affinities of the control compounds for AAG and albumin selected from the literature for assay validation were measured at 20−25 °C. However, compound affinity can be temperature dependent, so we also tested vismodegib binding at 37 °C to make a direct comparison with the clinical, equilibrium dialysis, and cellular inhibition experiments.

hAAG and rAAG surfaces were prepared using thiol coupling[20,21] because of the low isoelecric point and tested with biliverdin, which is thought to be an endogenous ligand for AAG.[22] Biliverdin binding has been characterized biophysically with a reported solution affinity for hAAG of 8.3 μM at 25 °C.[24] For biliverdin we noted two-site binding to both hAAG and rAAG (Figure 3B). The high-affinity site in hAAG was 15.3 μM (Table 2), in close agreement with the published value, whereas binding to rAAG was ~3-fold weaker, with a high-affinity site binding constant of 71.0 μM (Table 2). These results suggest that sequence differences between the two proteins may subtly influence the binding for biliverdin. Vismodegib was found to exhibit two-site binding to hAAG with a high-affinity site binding constant of 3.7 μM at 20 °C (Figure 3B, Table 2), even stronger than biliverdin. The affinity of vismodegib for hAAG is not strongly temperature dependent, with affinity at 37 °C lowering only 3-fold to 13 μM. This is fairly potent binding to AAG and may be a contributing factor to the observation that total vismodegib concentrations correlate strongly with total AAG concentrations in humans. SPR reveals that the vismodegib affinity for rAAG is 120 μM at 20 °C, which is more than 30-fold weaker than to the human protein (Figure 3B, Table 2) and undetectable at 37 °C at concentrations up to the compound solubility limit. This suggests that key residues involved in the vismodegib binding site are different between the two species. In addition, the time resolution of the experiment shows that the hAAG/vismodegib interaction is rapidly reversible with total dissocation from AAGs achieved in fewer than 5 s. Thus, vismodegib can rapidly exchange between the free and hAAG-bound states. This reversibility suggests that the complications arising from a slow AAG dissocation observed for some drugs[13] are likely not applicable to vismodegib.

HSA and RSA were coupled to biosensor chips using amine coupling and tested using warfarin as a standard. We observed two-site binding to HSA and RSA (Figure 3A), consistent with other biosensor measurements.[23] For HSA at 20 °C, high- and low-affinity site K_D values of 5.4 and 510 μM were observed (Table 2), in good agreement with previously reported measurements of 3.8 and 273 μM.[24] Warfarin binding to RSA was slightly weaker, with high- and low-affinity site K_D values of 20 and 900 μM (Table 2). Vismodegib binding to both albumins was tested and also exhibited two-site binding (Figure 3A). The high-affinity binding sites for HSA and RSA had K_D estimates of 6.0 and 5.8 μM, respectively (Table 2), indicating no species dependence in the binding of vismodegib to albumins. At 37 °C the affinity of warfarin was slightly reduced on HSA and RSA about 3- to 5-fold to 12 and 95 μM, respectively. The secondary binding site was no longer detectable, and only a single K_D is reported. In contrast, vismodegib binding was markedly impacted by temperature and affinity to HSA, and RSA was reduced ~120-fold to 120 and 140 μM, respectively, with no observable secondary binding. This affinity is consistent with an equilibrium dialysis measurement of HSA and vismodegib at 37 °C (data not shown). As in the case of AAG binding, vismodegib rapidly and completely dissociates from albumin in 1−2 s.

Affinity and Thermodynamic Characterization of the Interaction between Vismodegib, AAG, and Albumin. Because the observed protein binding results have important implications for semimechanistic PK models describing the PK properties of vismodegib, we sought to confirm the affinities determined by equilibrium binding and SPR and further elucidate the binding properties thermodynamically using ITC. hAAG, rAAG, and HSA were dialyzed overnight, and the final dialysis buffer was used to prepare stock solutions of vismodegib, biliverdin, and warfarin (see Experimental Section). A sample titration of vismodegib with hAAG is shown in Figure 4. Similar titrations were conducted with control compounds (see Experimental Section), and the resultant binding constants and thermodynamic data for all titrations are summarized in Table 3. The affinities determined by ITC correspond well with those from the temperature-matched SPR binding experiments. The measured affinity of vismodegib at 20 °C to rAAG is more than 100-fold weaker than that of hAAG (K_D of 118 ± 59 and 1.1 ± 0.6 μM, respectively) in agreement with the SPR results. It is interesting to note that vismodegib binding to either AAG protein is enthalpically driven, indicating that vismodegib likely makes favorable hydrogen bonding interactions in the binding pocket. By contrast, vismodegib binding to HSA at 20 °C is entropically driven, suggesting that hydrophobic interactions predominate. The biliverdin control shows similar entropic binding signatures for hAAG binding, whereas warfarin/HSA binding is dominated by enthalpic interactions. All measured pairings had overall favorable Gibbs free

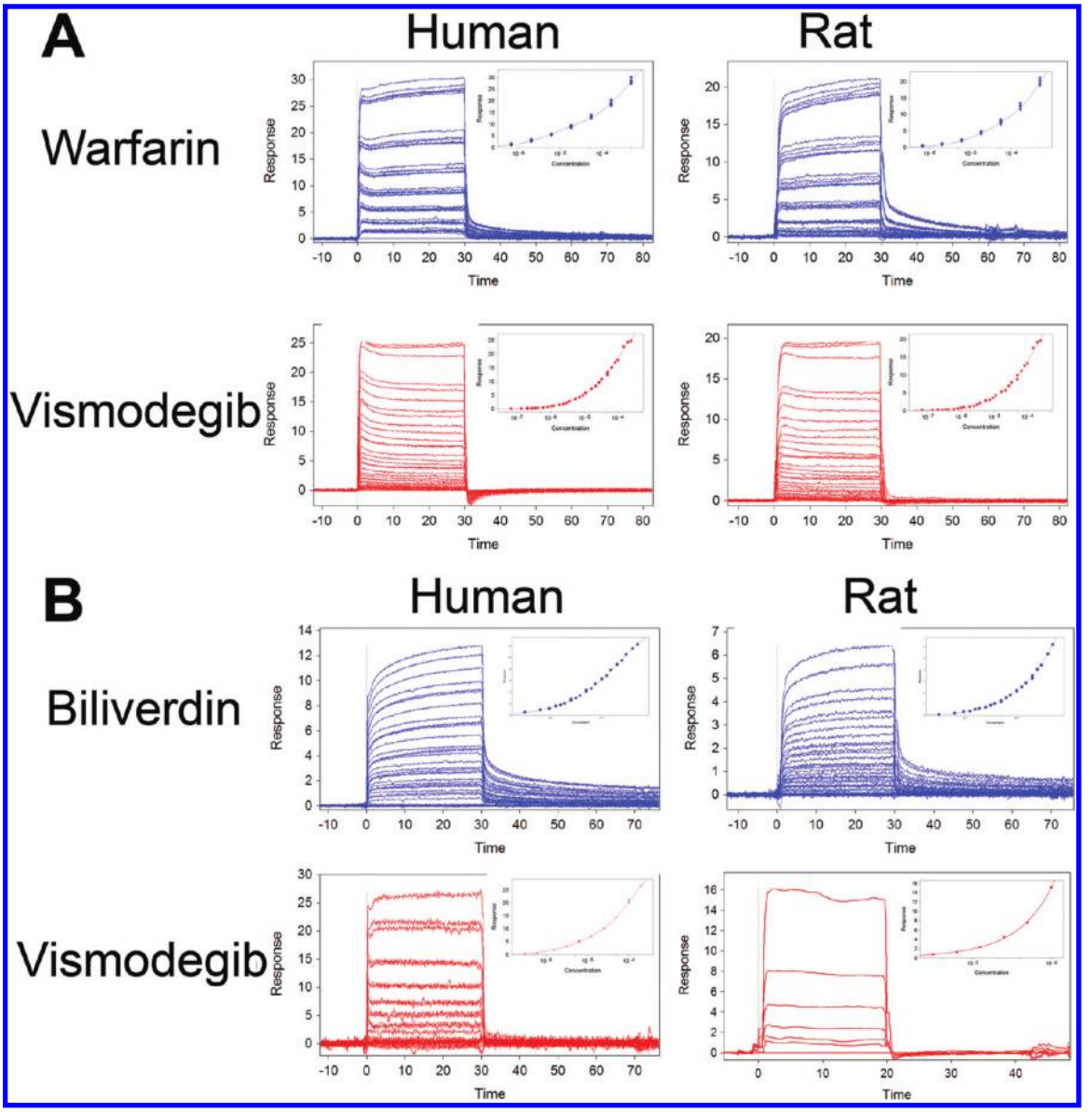

Figure 3. Binding of (A) warfarin and vismodegib to human and rat serum albumins and (B) biliverdin and vismodegib to human and rat α-1-acid glycoproteins. Sensorgrams are shown with time in seconds on the *X*-axis and binding response units on the *Y*-axis. The insets show the dose-response curves as the log of the concentration versus the measured response value averaged over two seconds before the end of the injection. Warfarin was measured in quadruplicate with a top concentration of 500 μM in a 3-fold dilution series. Vismodegib and biliverdin were measured using a cross-serial dilution strategy to minimize effects from insoluble compounds. Top concentrations for biliverdin and vismodegib are 500 and 250 μM, respectively.

Table 2. Equilibrium Binding Constants (K_D) Determined from Fitting the SPR Data Shown in Figure 3[a]

	K_D (μM)							
	temperature 37 °C				temperature 20 °C			
	AAG		albumin		AAG		albumin	
compd	human	rat	human	rat	human	rat	human	rat
vismodegib	13	NB	120	140	3.7, 139	120	6.0, 130	5.8, 171
warfarin	NB	NB	12	95	NB	NB	5.4, 510	20.0, 900
biliverdin			NB	NB	15.3, 219	71.0, 1700	NB	NB

[a] NB: nonbinding. Two K_D values are listed when a high-affinity and low-affinity binding event were observed.

dx.doi.org/10.1021/jm1008924 |*J. Med. Chem.* 2011, 54, 2592–2601

energies within a range of −5 to −8 kcal/mol. Because of the significant difficulty in preparing vismodegib solutions for ITC analysis (see methods section), the measurements were not repeated at the higher temperature or on RSA.

Computational Modeling of Vismodegib and Biliverdin Interaction with AAG. We have established that vismodegib exhibits markedly different binding to hAAG and rAAG but biliverdin does not, suggesting that these compounds may bind in different orientations to the protein in a way that would explain the experimental binding differences. The hAAG and rAAG amino acid sequences are 47% identical (68% similar), and approximately 14 residues differ between the two proteins in the first shell of residues that line the putative binding site based on our analysis of the crystal structure.[25] Although there are no reported experimental structures of compounds bound to AAG, we docked vismodegib to apo-AAG to determine whether the resulting poses would be consistent with the binding data.

The crystal structure of AAG has been solved, and the protein has been identified as a member of the lipocalin family (Figure 5A). Lipocalins bind compounds in the large cleft inside the β-barrel. AAG likely does as well, as evidenced by the presence of the N-terminal residues of another AAG molecule, a bound 2,3-dihydroxypropyl acetate molecule,[25] and binding and mutagenic studies.[26] Thus, we centered our docking studies in a large grid encompassing the entire cleft.

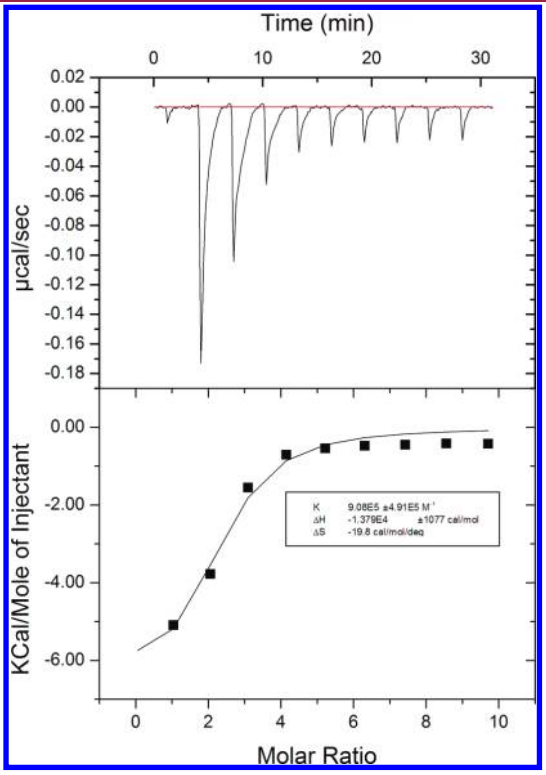

Figure 4. Thermodynamic profile of the interaction between vismodegib with hAAG.

Gold, version 4.1,[27] was used to dock vismodegib into the binding site of the hAAG and rAAG. For the human protein we used PDB code 3KQ0[25] after non-protein atoms were removed (see Experimental Section). For the rat isoform, a homology model was built using SWISS-MODEL.[28] For each protein, multiple docking runs of vismodegib consistently converged on a single binding mode, but the modes were significantly different between the human and rat proteins (Figure 5B and Figure 5C). Against the human protein (Figure 5B), vismodegib is predicted to adopt an extended conformation with the sulfonyl oxygens accepting hydrogen bonds from Tyr37 and His97 and the pyridyl nitrogen accepting a hydrogen bond from Tyr127. This is consistent with the enthalpic binding signature observed in the ITC experiments. Hydrophobic interactions between the aromatic rings of vismodegib and Phe32, Phe114, Tyr27, and Phe49 also contribute to binding.

By contrast, the rat protein is predicted to contain key residue differences in the binding site that result in a predicted 180° flip in compound binding (Figure 5C) relative to the mode observed in the human structure (Figure 5B). Specifically, a Thr47 (human) to Glu48 (rat) change results in a smaller binding cavity, which is predicted to be incompatible with the human-binding mode because of a significant steric clash, in addition to altering the local charge distribution. Furthermore, His97 (human) to Ile98 (rat) and Tyr37 (human) to Phe38 (rat) differences result in a loss of two potential hydrogen bonds to the sulfonyl oxygens of vismodegib and an increase in the hydrophobicity of this site. Multiple docking runs against the rat model consistently predicted a flipped orientation of vismodegib, with inhibitor pyridyl ring nestled in a hydrophobic cavity formed by Phe33, Phe38, Ile98, and Phe115. The sulfonyl group no longer has obvious hydrogen bonding interactions to stabilize the binding. Such an altered orientation and ligand conformation with few favorable contacts is consistent with the reduced affinity to the rAAG that is observed experimentally. The somewhat reduced composite Gold docking scores against the rat (55) versus human (61) proteins lend additional support to these observations.

For comparison, the docking of biliverdin to hAAG and rAAG was also examined (Figure 5D). Similar to vismodegib, biliverdin was docked near the large cleft. This is consistent with nuclear magnetic resonance studies on another lipocalin family member that shows biliverdin interacting with residues in the barrel and the helix connecting strands 1 and 2.[29] The results of docking experiments predict that billiverin has roughly similar binding orientations in hAAG and rAAG. Similar to the binding of biliverdin to phycocyanobilin:ferredoxin oxidoreductase protein from which the biliverdin structure was taken,[30] the hydrophobic face made from the ethylene and flanking methyl groups on the

Table 3. Equilibrium Binding Constants and Thermodynamic Parameters Determined from ITC

compd	protein	K_D (μM)	ΔG (kcal/mol)	ΔH (kcal/mol)	ΔS ((cal/mol)/deg)
vismodegib	hAAG	1.1 ± 0.6	−8.0 ± 1.1	−13.8 ± 1.1	−19.8
	rAAG	118.0 ± 59	−5.2 ± 2.0	−49.1 ± 2.0	−150.0
	HSA	5.5 ± 1.7	−7.0 ± 0.7	9.6 ± 0.7	56.8
biliverdin	hAAG	7.0 ± 5.0	−6.9 ± 0.1	0.3 ± 0.1	24.5
warfarin	HSA	2.0 ± 0.6	−7.6 ± 0.5	−9.5 ± 0.5	−6.4

dx.doi.org/10.1021/jm1008924 |J. Med. Chem. 2011, 54, 2592–2601

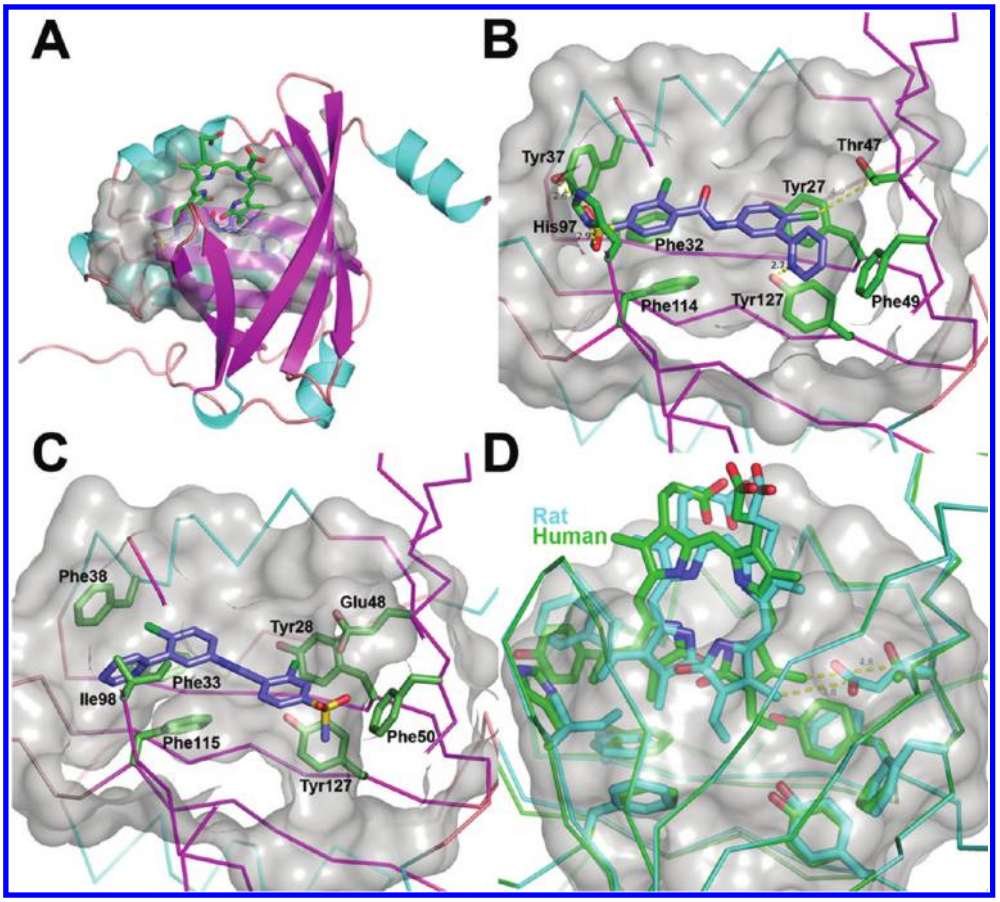

Figure 5. Docking models of vismodegib and biliverdin binding hAAG and rAAG. All figures were created using PyMol sofware (DeLano, W. L. *The PyMOL Molecular Graphics System*; DeLano Scientific: Palo Alto, CA; http://www.pymol.org. (software now available from Schrodinger, Inc., http://www.schrodinger.com). (A) Overall structure of hAAG from 3KQ0[24] demonstrating the lipocalin fold. Helices are colored blue, β-strands are magenta, and loops are pink. Vismodegib (light blue) and biliverdin (green) are superimposed on the structure based on docking to show the significantly different binding orientations for the two compounds. A semitransparent van der Waals surface of the protein is drawn around the compounds to show the extent and depth of the pocket. (B) Figure as in (A) but rotated around the *X*-axis and magnified to show vismodegib docked in the hAAG structure. Residues contacting the compound are shown as green sticks. Important hydrogen bonds from His97, Tyr37, and Tyr127 are shown. The van der Waals distance between Thr47 and the exocyclic chloro group on vismodegib indicate that changes in this amino acid position to larger side chains would not be sterically tolerated. (C) Figure as in (B) showing vismodegib docked into rAAG. The rat counterpart residues to the human shown in (B) are drawn as green sticks. No strong hydrogen bonds are predicted; the sulfonyl oxygens are buried in a relatively hydrophobic pocket. Note that Thr47 in hAAG (B) has been replaced by a Glu in the rat isoform, significantly constricting the active site in this area and causing a predicted 180° flip in vismodegib binding mode. (D) Superposition of the docked models of biliverdin to hAAG (green) and rAAG (cyan). Residues important to vismodegib binding are shown as sticks. Only the pyrrolidone group on the right side of the figure shows any significant difference between human and rat, likely due to the Thr47 (human)/Glu48 (rat) substitution. Distances from the pyrrolidone to the amino acid are shown in yellow.

terminal pyrrolidone rings is predicted to insert deep into the hydrophobic region of the active sites, making contacts with the Phe and Tyr aromatic residues. This is consistent with the ITC data that predict more hydrophobic interactions. The carboxyethyl groups extend out of the cavity into the solvent. The similar binding modes predicted for the human and rat proteins are consistent with the similarity in the observed affinities of biliverdin for both species. In the rAAG/biliverdin model, one of the terminal pyrrolidone rings is moved in toward the center of the cavity relative to the hAAG/biliverdin model, most likely because of the substitution of the nearby Thr47 (human) residue for a Glu48 (rat), which would clash sterically (Figure 5D). Other residue differences between the two species predicted to influence vismodegib binding do not make significant contacts with biliverdin (Figure 5D), consistent with binding data indicating similar affinities for both AAGs.

■ DISCUSSION AND CONCLUSIONS

To thoroughly understand the processes that lead to the atypical PK of vismodegib, we are conducting systematic evaluations of nonlinear absorption due to low solubility and slow metabolic elimination and report here on the experimental studies of plasma protein binding. Most drugs exhibit some degree of protein binding, and a wide range of affinities to various plasma proteins can be tolerated without adverse effect on the in vivo efficacy of the compound. However, a high degree of plasma protein binding can unfavorably influence both efficacy and the disposition of compounds.[11−13] Vismodegib, a first-in-class inhibitor of Hh signaling, is highly protein bound in plasma and has an unexpectedly high plasma exposure and long half-life in humans.[7,8] In addition, total vismodegib and AAG plasma concentrations in patients are strongly correlated, suggesting that protein binding influences drug disposition. We initiated detailed studies of

vismodegib binding to AAG and albumin to characterize the effect of each of these proteins and utilized proteins from humans and rats in an attempt to gain insights into PK differences in the two species. Results from the studies reported herein were instrumental to develop and inform a semimechanistic PK model which will be used in conjunction with clinical trial results to determine the optimal vismodegib dose and schedule.

On the basis of the vismodegib/AAG concentration correlation in patients, equilibrium dialysis at multiple drug and hAAG concentrations was performed and demonstrated both a high percent-binding and strong binding affinity to hAAG. Consistent with the free drug hypothesis, we assumed that only free drug could cross the cell membrane and result in a pharmacological effect; however, the formal possibility remained that the drug/protein complex could be active if vismodegib were to bind to an extracellular region of SMO (i.e., $K_D(SMO) \gg K_D(AAG)$). To establish that only free drug, and not drug/protein complex, is capable of inhibiting Hh signaling, in vitro cellular inhibition assays were performed with increasing concentrations of hAAG. These experiments showed that hAAG reduces the apparent IC_{50} of vismodegib for inhibiton of Hh signaling. However, at concentrations of hAAG in the range observed in cancer patients (Figure 1) there is sufficient free compound available to significantly attenuate hH signaling, and activity is totally inhibited only when the hAAG concentrations exceed those observed in patients. The demonstrated efficacy of the drug in advanced basal cell carcinoma in a phase 1 clinical trial is consistent with the ability of vismodegib to inhibit Hh signaling in the presence of plasma AAG in these patients.[31]

Given the observed binding affinity to hAAG, observed species differences in PK parameters, and the possible additional HSA-mediated contributions to protein binding, we initiated biophysical binding experiments using SPR and ITC to evaluate the interactions with human and rat AAGs and albumins in detail. Both methods confirmed the low micromolar binding of vismodegib to hAAG and demonstrated a dramatically reduced affinity for rAAG. While both methods also reveal low micromolar binding to albumin at 20 °C, there is significant affinity loss observed with an increase to physiological temperature observed by SPR and equilibrium dialysis. Additionally, all binding is rapidly and completely reversible. Taken together, these data suggest that as compound enters the bloodstream, it will preferentially bind to available binding sites on AAG. Albumin, being lower affinity but having higher capacity, is then able to bind residual drug, keeping vismodegib at a low and constant free fraction consistent with clinically observed results (data not shown).

The binding profile of vismodegib to AAG, including a large species dependence of binding, is somewhat reminiscent of UCN-01, which exhibits strong species-dependent binding to hAAG, has a reduced volume of distribution, and has a long serum half-life in patients relative to preclinical species.[13] The reduction in volume of distribution was ascribed to the potent binding of UCN-01 to AAG, whereas the long half-life has been attributed to a slow/irreversible off-rate from hAAG that keeps it sequestered from target interaction or metabolic clearance. Unlike UCN-01, vismodegib's rapid dissociation from plasma proteins suggests that, whereas a large fraction of the compound will be bound to plasma proteins, there will be a constant free fraction available to clearance mechanisms and tissues. Although the drug will be protein bound most of the time, perhaps affecting total clearance, the rapid reversibility would likely prevent the binding from affecting elimination driven by intrinisic metabolic clearance (i.e., of free drug). Thus, species differences in AAG binding may partially contribute to the prolonged half-life in humans relative to rats, but these data indicate that differences in metabolic clearance of vismodegib in rats relative to humans play a significant role in the half-life differences.

On the basis of insights gained from the described studies on the unique species specific binding of vismodegib to AAG, we propose that there is added value in collecting biophysical data earlier in the lead and candidate optimization processes. Rapid characterization of the binding of xenobiotics to plasma proteins, and the ultimate goal of identifying compounds with optimal free drug levels needed for efficacy, has long been a challenge to the medicinal chemist during optimization. Part of this challenge is the difficulty in obtaining high throughput and quantitative binding to plasma proteins over a wide dynamic range. Use of biophysical techniques with dynamic ranges from the subnanomolar to the millimolar, such as those described in this manuscript, could be particularly important for therapeutic areas where there are known fluctuations in AAG levels in patients and in therapeutic areas where efficacy at the target organ is improved with higher levels of free drug. The throughputs of biophysical assays are such that they allow for examinations of binding of tens (ITC) to hundreds (SPR) of compounds per day, and for SPR, across multiple proteins from multiple species in parallel. Such rapid generation of data enables SAR of analogues against specific plasma proteins such as albumin or AAG. SAR derived from rapid analogue testing in SPR assays along with thermodynamic measurements from ITC and computational docking predictions could potentially provide testable hypotheses on how to develop analogues with altered binding properties to plasma proteins of interest and enable selection of compounds with optimal free concentrations. We do caution that such data may be complex and somewhat unpredictable because of the observed phenomenon that sometimes small changes to the compound can cause a reorientation in the binding pocket. AAG and albumin have broad open binding sites, often with multiple subpockets or channels that can favor different binding orientations of closely related molecules. For example, crystal stuctures in serum albumin of oxyphenbutazone and phenylbutazone, which differ by only a hydroxyl group, are flipped 180° relative to each other in the same binding pocket.[32] Thus, the throughput of the techniques can also be used for rapid scanning of analogues in search of a weaker plasma protein binder or as a way to differentiate between early lead series. In addition, measuring binding affinity and understanding molecular docking of compound analogs for multiple plasma proteins and multiple species can provide important mechanistic insights into species differences in drug disposition and activity. An understanding of these differences could be useful in enabling the translation of efficacy and/or safety in preclinical models to humans. For example, we are exploring incorporation of the information on species differences in plasma protein binding resulting from the described studies into PK simulations and human dose predictions with the goal of improving translation of preclinical data and reducing attrition of drug candidates during the clinical phase of a program.

EXPERIMENTAL SECTION

Reagents and Cell Lines. Vismodegib[6] and octyl modified human Shh[33] were produced at Genentech as described. Vismodegib purity was

determined to be 98% pure by HPLC. hAAG was purchased from Sigma (catalog no. G9885), and the S12 cell line was used as described previously.[3]

Vismodegib Analytical Method. Vismodegib plasma concentrations were determined using a validated solid-phase extraction liquid chromatographic−tandem mass spectrometry method, using reverse-phase chromatography coupled with a turbo ion spray interface validated over the calibration range of 5−5000 ng/mL (0.012—11.9 μM).[8]

AAG Analytical Methods. Concentrations of AAG in human K2-EDTA plasma were determined using a commercially available kit (Dade Behring Marburg GmbH, Marburg, Germany) modified for assay using a 96-well enzyme-linked immunosorbent assay.

Equilibrium Dialysis. An assessment of vismodegib binding to AAG was performed by equilibrium dialysis using an HTDialysis system (HTDialysis LLC, Gales Ferry, CT, U.S.) and radiolabeled [^{14}C]-vismodegib (Selcia Ltd., Essex, U.K.). Binding to AAG was assessed at vismodegib concentrations of 5, 25, and 75 μM and AAG concentrations of 0.5, 1, and 5 mg/mL. Briefly, [^{14}C]vismodegib and unlabeled vismodegib (Genentech Inc., South San Francisco, CA, U.S.) were added to AAG prepared at the indicated concentrations to achieve vismodegib concentrations of 5, 25, and 75 μM. Samples were equilibrated with 0.133 M isotonic phosphate buffer for 6 h at 37 °C in 5% CO_2 and 90% humidity. Radioactivity in postdialysis buffer and plasma was measured using a Packard Tri-Carb 2900TR liquid scintillation counter (Boston, MA, U.S.). The percent free fraction in each AAG sample was calculated by dividing the radiation in the postdialysis buffer side with the radiation in the postdialysis plasma side and multiplying by 100. The percent bound was calculated as 100 minus the percent free. Bound and free concentrations of vismodegib in each sample were calculated by multiplying the total vismodegib incubation concentration by the percent bound and free fractions of vismodegib, respectively. The K_D of AAG at the high-affinity AAG binding site was estimated by fitting vismodegib bound and free concentrations from AAG experiments to a two-site binding model using SAAM II (Saam Institute, University of Washington, Seattle, WA, U.S.), described as follows:

$$C_{bound} = \frac{B_{max1} C_u}{K_{d1} + C_u} + \frac{B_{max2}}{K_{d2}} C_u$$

where C_{bound} is the bound vismodegib concentration, C_u is the free vismodegib concentration, B_{max1} is the maximum binding capacity of the high-affinity site of vismodegib on AAG (value fixed as the AAG incubation concentration), B_{max2}/K_{D2} is the ratio of the maximum binding capacity and the dissociation rate constant of the low-affinity site of vismodegib on AAG, and K_{D1} is the dissociation constant of the high-affinity saturable site of vismodegib on AAG.

Luciferase Reporter Assay. S12 cells were seeded into six-well plates at 1.85 × 10^5 cells/well in high-glucose Dulbecco's modified Eagle's medium with 4 mM glutamine, 10 mM Hepes (pH 7.2), and 10% fetal bovine serum (FBS). Twenty-four hours later, cells were collected by trypsin treatment and each well was redistributed over four wells of a 12-well plate. The FBS content of the culture medium was reduced to 0.5% the following morning to induce formation of primary cilia. Shh, hAAG, and vismodegib were added at the indicated concentrations. Luciferase activity was determined 48 h later with the Dual-Glo luciferase assay system (Promega, catalog no. E2940) using an EnVision 2103 multilabel reader (Perkin-Elmer). Values shown are the mean of four separate experiments ± 1 standard deviation.

SPR Binding Experiments. SPR-based binding experiments were performed using a Biacore T100 or T200 instrument (GE Healthcare). Interactions were measured between a protein immobilized on a biosensor chip and a compound flowed over the surface. Response in resonance units (RU) was measured in real time at 10 Hz.[19,34] Human, rat, and mouse albumin, hAAG, and warfarin were purchased from Sigma. Biliverdin was purchased from MP Biomedicals, and rAAG was from Calbioreagents. Mock surfaces were also prepared by performing the immobilization procedures on a surface but without the addition of protein. The two albumins were coupled to series S CM5 sensor chips (GE Healthcare) using standard amine coupling protocols.[33] Briefly, after preconditioning the surfaces with short injections of NaOH, HCl, SDS, and H_3PO_4 and normalized, surfaces were activated with NHS/EDC for 7 min at 30 μL/min. Albumin diluted to 50 μg/mL in 10 mM sodium acetate buffer (pH 5) was injected across individual flow cells at 10 μL/min until 9000−13000 RU of protein was immobilized. Surfaces were then blocked with two 30 s injections of ethanolamine. Because of its low isoelectric point, AAG cannot be immobilized using amine coupling as above, and sensor surfaces were therefore prepared using the thiol coupling kit (GE Healthcare) and 2-[2-pyridinyldithio]ethaneamine. Briefly, hAAG, rAAG, and the surface of a CM5 sensor chip were modified to introduce a free thiol on the protein and the sensor surface. Protein was immobilized by a thiol-exchange reaction to a coupling density of 5000−6000 RU. Compounds were prepared as 10 mM stocks and diluted in dimethylsulfoxide (DMSO) to 20 times the top concentration desired in the experiment and then 20-fold into the running buffer to yield the compound in 50 mM Hepes (pH 7.2), 150 mM NaCl, 0.005% Tween-20, and 5% DMSO. In experiments where one albumin and one AAG were coupled on the same chip, reference flow cells were mock coupled by either amine or thiol coupling as appropriate. We found that the reference sensorgrams varied slightly between surfaces prepared by the two methods, and data reduction was performed using the appropriate reference surface. Experiments were run at either 20 or 37 °C, and no surface regeneration strategies were necessary. Raw sensorgram data were reduced, and solvent was corrected, double referenced, and fit using Scrubber II (BioLogic Software, Campbell, Australia; http://www.biologic.com/au). Equilibrium-binding fits were performed by averaging the response value over the last 1 s of the association phase and plotted against the concentration. Single-site or two-site models were used as appropriate.

ITC. Lyophilized powder stocks of hAAG and HSA (Sigma) were dissolved into sample buffer (50 mM HEPES [pH 7.2], 150 mM NaCl, 0.005% Tween-20, and 5% DMSO), and the resulting 300 μM hAAG and HSA samples, as well as a 100 μM rAAG (Calbioreagents) stock, were transferred to individual 6−8 kDa molecular weight cutoff D-tube dialyzers (Novagen) and dialyzed against 1 L of sample buffer overnight at 4 °C. After dialysis, the protein samples were transferred to Eppendorf tubes and stored at 4 °C unless otherwise specified. The remaining dialysis buffer was reserved for sample dilutions, control titrations, and the preparation of 300 μM biliverdin and warfarin stocks. The limited solubility of vismodegib under these conditions only allowed the preparation of a 6 μM vismodegib stock solution. Solid vismodegib was resuspended in dialysis buffer and sonicated intermittently overnight in a water bath at 38 °C. Undissolved solid was pelleted by repeated centrifugation at 20000g for 10 min at room temperature and the supernatant transferred to a new tube for each spin. By use of a standard quantitative assay[8] the concentration of vismodegib in the final soluble stock was determined to be 6 μM. All protein and compound samples were brought to 19 °C and degassed just prior to use. Titrations were performed using a MicroCal ITC200 calorimeter (GE Healthcare) at 20 °C with injections of 1.7−4.0 μL spaced at 3 min intervals. Aliquots of the 6 μM vismodegib solution were transferred to the sample chamber and titrated to saturation with each of the concentrated, dialyzed protein stock solutions. The stirred cell contained 6−25 μM compound, and the syringe held 100−300 μM protein. Additional titrations were conducted with 25−300 μM protein in the cell and 300−3000 μM compound in the syringe, where compound solubility permitted. The titration data were corrected for small heat changes observed in control titrations of sample stock solutions into buffer alone and fitted to a one-site model using Origin software, version 7.0552 (www.OriginLab.com).

Docking Studies. The hAAG protein structure 3KQ0 from the PDB[25] was used for docking. Water and dihydroxypopyl acetate were removed, and all hydrogens were added. For rAAG, a homology model

was built using SWISS-MODEL.[28] Vismodegib was built in an extended conformation in Sybyl, version 8.1 (Tripos), and minimized. Gold, version 4.1,[27] was used for all docking studies. Twenty poses were generated in all docking runs. The default Gold scoring function was used, with no rescoring and no constraints added. Gold was allowed to adjust protein but not ligand atom types. The protein structure was held fixed; however, the default Gold implementation examines flips of the ends of protein side chains to optimize ligand−protein hydrogen bonds. All dockings generated self-consistent binding modes, with <1.5 Å root-mean-square deviation differences in ligand heavy atom positions across all poses observed.

The structure of biliverdin IXα was obtained from a 1.5 Å X-ray structure of this ligand complexed to phycocyanobilin/ferredoxin oxidoreductase (2D1E in the PDB).[29] The amino acid sequence of this protein is not similar to that of AAG, but the protein presents an active site similar in size and shape to that of AAG. Biliverdin was manually placed in the large binding cleft of the hAAG and rAAG enzymes, orienting the hydrophobic face of the ligand made up from the ethylene and flanking methyl groups on the terminal pyrrolidone rings deep in the hydrophobic portion of the active site, and minimized from there along with residues within an 8 Å radius from the inhibitor. Biliverdin was also flipped 180° and minimized; the orientations shown in Figure 5 are the lowest energy versions. Docking using Gold (same options as were used for vismodegib) also reproduced the conformations shown in Figure 5 within 1.5 Å of the minimized versions.

AUTHOR INFORMATION

Corresponding Author

*Phone: 650-225-5791. Fax: 650-742-5167. E-mail: graham.richard@gene.com.

ACKNOWLEDGMENT

We thank the vismodegib phase I investigators Dr. Daniel Von Hoff, Dr. Patricia LoRusso, and Dr. Charles Rudin and the patients that enrolled in the clinical trial, spending valuable time away from their personal lives to advance science. Under the ongoing collaboration agreement between Genentech, a wholly owned member of the Roche Group, and Curis, vismodegib was discovered by Genentech and was jointly validated through a series of preclinical studies. Through this collaboration, Genentech and Roche are responsible for the clinical development and commercialization of vismodegib.

ABBREVIATIONS USED

SPR, surface plasmon resonance; ITC, isothermal titration calorimetry; AAG, α-1-acid glycoprotein; hAAG, human α-1-acid glycoprotein; rAAG, rat α-1-acid glycoprotein; HSA, human serum albumin; RSA, rat serum albumin; K_D, equilibrium binding dissociation constant; SMO, Smoothened protein; SAR, structure−activity relationship; HPLC, high performance liquid chromatography; EDTA, ehtylenediaminetatraacetic acid; SDS, sodium dodecyl sulfate; NHS, *N*-hydroxysuccinimide; EDC, 1-ethyl-3-(3-dimethylaminopropyl)carbodiimide; PK, pharmacokinetics; PD, pharmacodynamics

REFERENCES

(1) Ingham, P. W.; McMahon, A. P. Hedgehog signaling in animal development: paradigms and principles. *Genes Dev.* **2001**, *15* (23), 3059–3087.

(2) Rubin, L. L.; de Sauvage, F. J. Targeting the Hedgehog pathway in cancer. *Nat. Rev. Drug Discovery* **2006**, *5* (12), 1026–1033.

(3) Frank-Kamenetsky, M.; Zhang, X. M.; Bottega, S.; Guicherit, O.; Wichterle, H.; Dudek, H.; Bumcrot, D.; Wang, F. Y.; Jones, S.; Shulok, J.; Rubin, L. L.; Porter, J. A. Small-molecule modulators of Hedgehog signaling: identification and characterization of Smoothened agonists and antagonists. *J. Biol.* **2002**, *1* (2), 10.

(4) Marsters, J. C. Small Molecule Antagonists of the Hedgehog Pathway. Presented at the Annual Meeting of the American Association of Cancer Research, San Diego, CA, April 12−16, 2008.

(5) Yauch, R. L.; Dijkgraaf, G. J.; Alicke, B.; Januario, T.; Ahn, C. P.; Holcomb, T.; Pujara, K.; Stinson, J.; Callahan, C. A.; Tang, T.; Bazan, J. F.; Kan, Z.; Seshagiri, S.; Hann, C. L.; Gould, S. E.; Low, J. A.; Rudin, C. M.; de Sauvage, F. J. Smoothened mutation confers resistance to a Hedgehog pathway inhibitor in medulloblastoma. *Science* **2009**, *326* (5952), 572–574.

(6) Robarge, K. D.; Brunton, S. A.; Castanedo, G. M.; Cui, Y.; Dina, M. S.; Goldsmith, R.; Gould, S. E.; Guichert, O.; Gunzner, J. L.; Halladay, J.; Jia, W.; Khojasteh, C.; Koehler, M. F.; Kotkow, K.; La, H.; Lalonde, R. L.; Lau, K.; Lee, L.; Marshall, D.; Marsters, J. C., Jr.; Murray, L. J.; Qian, C.; Rubin, L. L.; Salphati, L.; Stanley, M. S.; Stibbard, J. H.; Sutherlin, D. P.; Ubhayaker, S.; Wang, S.; Wong, S.; Xie, M. GDC-0449, a potent inhibitor of the Hedgehog pathway. *Bioorg. Med. Chem. Lett.* **2009**, *19* (19), 5576–5581.

(7) Wong, H.; Chen, J. Z.; Chou, B.; Halladay, J. S.; Kenny, J. R.; La, H.; Marsters, J. C.; Plise, E.; Rudewicz, P. J.; Robarge, K.; Shin, Y.; Wong, S.; Zhang, C.; Khojasteh, S. C. Preclinical assessment of the absorption, distribution, metabolism and excretion of GDC-0449 (2-chloro-*N*-(4-chloro-3-(pyridin-2-yl)phenyl)-4-(methylsulfonyl)benzamide) , an orally bioavailable systemic Hedgehog signalling pathway inhibitor. *Xenobiotica* **2009**, *39*, 850–861.

(8) Ding, X.; Chou, B.; Graham, R. A.; Cheeti, S.; Percey, S.; Matassa, L. C.; Reuschel, S. A.; Meng, M.; Liu, S.; Voelker, T.; Lum, B. L.; Rudewicz, P. J.; Hop, C. E. Determination of GDC-0449, a small-molecule inhibitor of the Hedgehog signaling pathway, in human plasma by solid phase extraction-liquid chromatographic−tandem mass spectrometry. *J. Chromatogr., B: Anal. Technol. Biomed. Life Sci.* **2010**, *878* (9−10), 785–790.

(9) Urien, S.; Barre, J.; Morin, C.; Paccaly, A.; Montay, G.; Tillement, J. P. Docetaxel serum protein binding with high affinity to alpha 1-acid glycoprotein. *Invest. New Drugs* **1996**, *14* (2), 147–151.

(10) Lu, J. F.; Eppler, S. M.; Wolf, J.; Hamilton, M.; Rakhit, A.; Bruno, R.; Lum, B. L. Clinical pharmacokinetics of erlotinib in patients with solid tumors and exposure−safety relationship in patients with non-small cell lung cancer. *Clin. Pharmacol. Ther.* **2006**, *80* (2), 136–145.

(11) Li, J.; Brahmer, J.; Messersmith, W.; Hidalgo, M.; Baker, S. D. Binding of gefitinib, an inhibitor of epidermal growth factor receptor-tyrosine kinase, to plasma proteins and blood cells: in vitro and in cancer patients. *Invest. New Drugs* **2006**, *24* (4), 291–297.

(12) Delbaldo, C.; Chatelut, E.; Re, M.; Deroussent, A.; Seronie-Vivien, S.; Jambu, A.; Berthaud, P.; Le Cesne, A.; Blay, J. Y.; Vassal, G. Pharmacokinetic−pharmacodynamic relationships of imatinib and its main metabolite in patients with advanced gastrointestinal stromal tumors. *Clin. Cancer Res.* **2006**, *12* (20 Part 1), 6073–6078.

(13) Fuse, E.; Kuwabara, T.; Sparreboom, A.; Sausville, E. A.; Figg, W. D. Review of UCN-01 development: a lesson in the importance of clinical pharmacology. *J. Clin. Pharmacol.* **2005**, *45* (4), 394–403.

(14) Fuse, E.; Tanii, H.; Takai, K.; Asanome, K.; Kurata, N.; Kobayashi, H.; Kuwabara, T.; Kobayashi, S.; Sugiyama, Y. Altered pharmacokinetics of a novel anticancer drug, UCN-01, caused by specific high affinity binding to alpha1-acid glycoprotein in humans. *Cancer Res.* **1999**, *59* (5), 1054–1060.

(15) Trainor, G. L. The importance of plasma protein binding in drug discovery. *Expert Opin. Drug Discovery* **2007**, *2* (1), 51–64.

(16) Israili, Z. H.; Dayton, P. G. Human alpha-1-glycoprotein and its interactions with drugs. *Drug Metab. Rev.* **2001**, *33* (2), 161–235.

(17) Holladay, J. W.; Dewey, M. J.; Michniak, B. B.; Wiltshire, H.; Halberg, D. L.; Weigl, P.; Liang, Z. M.; Halifax, K.; Lindup, W. E.; Back, D. J. Elevated alpha-1-acid glycoprotein reduces the volume of

distribution and systemic clearance of saquinavir. *Drug Metab. Dispos.* **2001**, *29* (3), 299–303.

(18) Zsila, F.; Fitos, I.; Bencze, G.; Keri, G.; Orfi, L. Determination of human serum alpha(1)-acid glycoprotein and albumin binding of various marketed and preclinical kinase inhibitors. *Curr. Med. Chem.* **2009**, *16* (16), 1964–1977.

(19) Malmqvist, M. Biospecific interaction analysis using biosensor technology. *Nature* **1993**, *361* (6408), 186–187.

(20) Frostell-Karlsson, A.; Remaeus, A.; Roos, H.; Andersson, K.; Borg, P.; Hamalainen, M.; Karlsson, R. Biosensor analysis of the interaction between immobilized human serum albumin and drug compounds for prediction of human serum albumin binding levels. *J. Med. Chem.* **2000**, *43* (10), 1986–1992.

(21) Day, Y. S.; Baird, C. L.; Rich, R. L.; Myszka, D. G. Direct comparison of binding equilibrium, thermodynamic, and rate constants determined by surface- and solution-based biophysical methods. *Protein Sci.* **2002**, *11* (5), 1017–25.

(22) Zsila, F.; Mady, G. Biliverdin is the endogenous ligand of human serum alpha(1)-acid glycoprotein. *Biochem. Biophys. Res. Commun.* **2008**, *372* (3), 503–507.

(23) Day, Y. S. N.; Myszka, D. G. Characterizing a drug's primary binding site on albumin. *J. Pharm. Sci.* **2003**, *92* (2), 333–343.

(24) Rich, R. L.; Day, Y. S. N.; Morton, T. A.; Myszka, D. G. High-resolution and high-throughput protocols for measuring drug/human serum albumin interactions using BIACORE. *Anal. Biochem.* **2001**, *296* (2), 197–207.

(25) Schonfeld, D. L.; Ravelli, R. B. G.; Mueller, U.; Skerra, A. The 1.8-angstrom crystal structure of alpha(1)-acid glycoprotein (orosomucoid) solved by UV RIP reveals the broad drug-binding activity of this human plasma lipocalin. *J. Mol. Biol.* **2008**, *384* (2), 393–405.

(26) Zsila, F.; Iwao, Y. The drug binding site of human alpha(1)-acid glycoprotein: insight from induced circular dichroism and electronic absorption spectra. *Biochim. Biophys. Acta, Gen. Subj.* **2007**, *1770* (5), 797–809.

(27) Jones, G.; Willett, P.; Glen, R. C.; Leach, A. R.; Taylor, R. Development and validation of a genetic algorithm for flexible docking. *J. Mol. Biol.* **1997**, *267* (3), 727–748.

(28) Arnold, K.; Bordoli, L.; Kopp, J.; Schwede, T. The SWISS-MODEL workspace: a Web-based environment for protein structure homology modelling. *Bioinformatics* **2006**, *22* (2), 195–201.

(29) Miyamoto, Y.; Nishimura, S.; Inoue, K.; Shimamoto, S.; Yoshida, T.; Fukuhara, A.; Yamada, M.; Urade, Y.; Yagi, N.; Ohkubo, T.; Inui, T. Structural analysis of lipocalin-type prostaglandin D synthase complexed with biliverdin by small-angle X-ray scattering and multidimensional NMR. *J. Struct. Biol.* **2010**, *169* (2), 209–218.

(30) Hagiwara, Y.; Sugishima, M.; Takahashi, Y.; Fukuyama, K. Crystal structure of phycocyanobilin: ferredoxin oxidoreductase in complex with biliverdin IX alpha, a key enzyme in the biosynthesis of phycocyanobilin. *Proc. Natl. Acad. Sci. U.S.A.* **2006**, *103* (1), 27–32.

(31) Von Hoff, D. D.; LoRusso, P. M.; Rudin, C. M.; Reddy, J. C.; Yauch, R. L.; Tibes, R.; Weiss, G. J.; Borad, M. J.; Hann, C. L.; Brahmer, J. R.; Mackey, H. M.; Lum, B. L.; Darbonne, W. C.; Marsters, J. C.; de Sauvage, F. J.; Low, J. A. Inhibition of the Hedgehog pathway in advanced basal-cell carcinoma. *N. Engl. J. Med.* **2009**, *361* (12), 1164–1172.

(32) Ghuman, J.; Zunszain, P. A.; Petitpas, I.; Bhattacharya, A. A.; Otagiri, M.; Curry, S. Structural basis of the drug-binding specificity of human serum albumin. *J. Mol. Biol.* **2005**, *353* (1), 38–52.

(33) Taylor, F. R.; Wen, D. Y.; Garber, E. A.; Carmillo, A. N.; Baker, D. P.; Arduini, R. M.; Williams, K. P.; Weinreb, P. H.; Rayhorn, P.; Hronowski, X. P.; Whitty, A.; Day, E. S.; Boriack-Sjodin, A.; Shapiro, R. I.; Galdes, A.; Pepinsky, R. B. Enhanced potency of human sonic Hedgehog by hydrophobic modification. *Biochemistry* **2001**, *40* (14), 4359–4371.

(34) Johnsson, B.; Lofas, S.; Lindquist, G. Immobilization of proteins to a carboxymethyldextran-modified gold surface for biospecific interaction analysis in surface-plasmon resonance sensors. *Anal. Biochem.* **1991**, *198* (2), 268–277.